PLASMA PHYSICS GROUP

A Unified Theory of SAR Arc Formation at the Plasmapause

John M. Cornwall, F. V. Coroniti, and R. M. Thorne

November, 1970 R-82

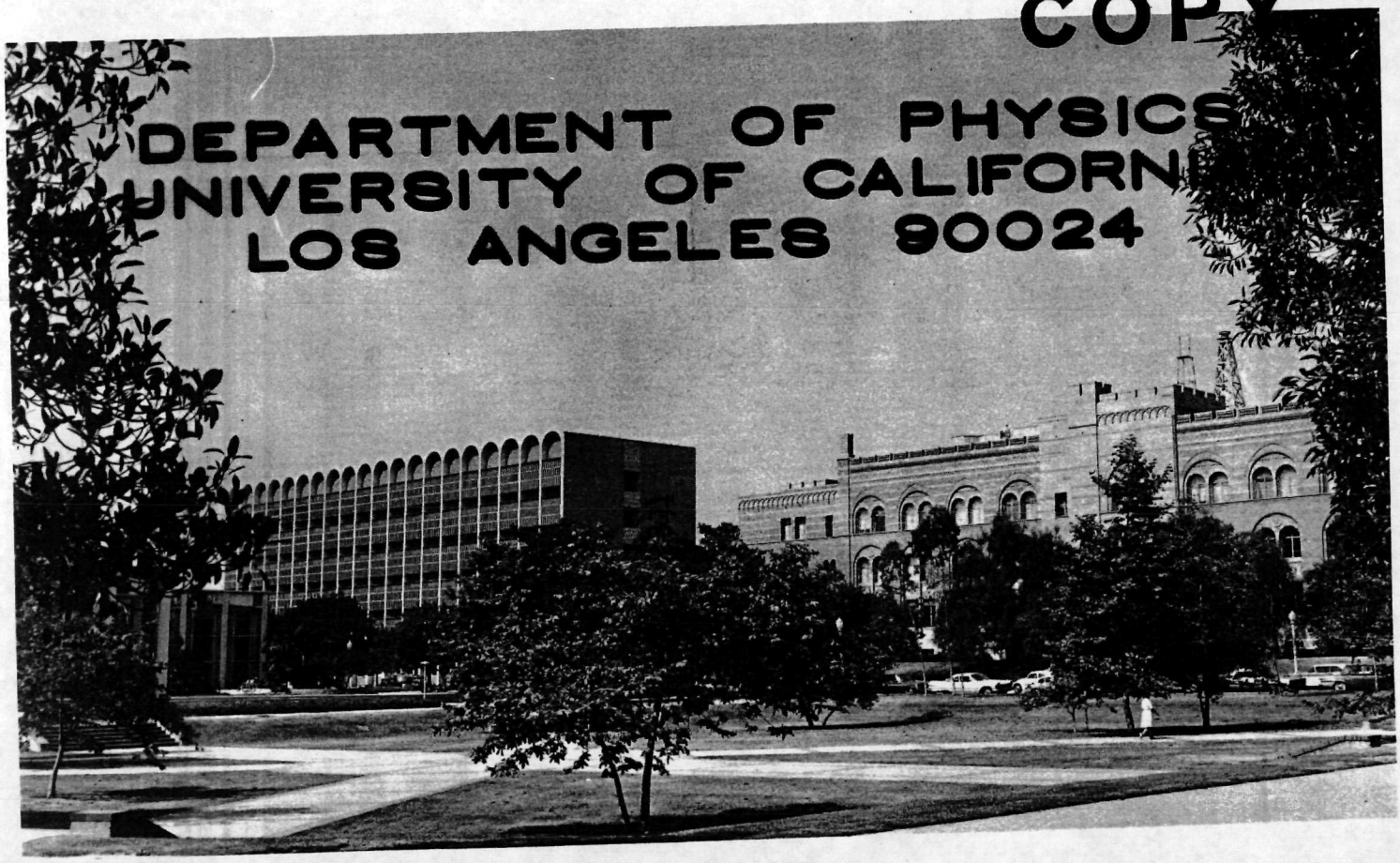

A Unified Theory of SAR Arc Formation at the Plasmapause

John M. Cornwall, F. V. Coroniti, and R. M. Thorne

November, 1970 R-82

A Unified Theory of SAR Arc Formation at the Plasmapause

John M. Cornwall,[1] F. V. Coroniti,[2] and R. M. Thorne[3]

ABSTRACT

We propose that SAR-arcs are generated at the plasmapause as a consequence of the turbulent dissipation of ring current energy. During the recovery phase of a geomagnetic storm, the plasmapause expands outward into the symmetric ring current. When the cold plasma densities reach about 100 cm^{-3}, ring current protons ($E_p \sim 20$ keV) become unstable and generate intense ion cyclotron wave turbulence in a narrow region 1/2 R_e wide (just inside the plasmapause). Approximately one-half of the ring current energy is dissipated into wave turbulence which in turn is absorbed through a Landau resonant interaction with plasmaspheric electrons. The combined thermal heat flux to the ionosphere due to Landau absorption of the wave energy and proton-electron Coulomb dissipation is sufficient to drive SAR-arcs at the observed intensities. We thus predict that the arcs should be localized to a narrow latitudinal range just within the stormtime plasmapause. They should occur at all local times and persist for the 10 to 20 hour duration of the plasmapause expansion. Expected proton precipitation fluxes will not contaminate the spectral purity of SAR-arcs.

---

1. Department of Physics, University of California at Los Angeles (permanent address), and Aerospace Corporation, El Segundo, California 90045.

2. Department of Physics, University of California at Los Angeles 90024.

3. Department of Meteorology, University of California at Los Angeles 90024.

1.0 INTRODUCTION

Over the past several years a consensus has arisen that stable auroral red arcs (SAR-ARCS) are excited by the conduction of heat from magnetospheric electrons to the red arc ionospheric region. Furthermore, the pioneering papers of Cole [1964; 1965; 1967] have established that the ring current protons are an adequate SAR-arc energy source. The major remaining fundamental theoretical uncertainty is the conversion of proton energy into electron heat.

Cole [1965] originally formulated the transfer process as proton energy degradation via Coulomb collisions with cool plasmaspheric electrons. Recent experimental and theoretical work, however, suggests that proton Coulomb dissipation alone may be inadequate for supplying the required SAR-arc electron heating rates: First, the storm-time ring current proton energy spectrum peaks between 10 and 50 KeV [Frank, 1967; Frank and Owens, 1970]. Coulomb dissipation rates appropriate for these energies are considerably lower than Cole's original estimate which was based on a mean proton energy of 1 KeV. Second, satellite observations by Chappell, et al., [1970] have demonstrated a strong correlation between the SAR-arc latitudinal location and the plasmapause. Similarly, several ground based observations have shown that SAR-arcs are spatially correlated with the equatorial edge of the ionospheric trough [Clark, et al., 1969; Norton and Findlay, 1969; Norton and Marovich, 1969; Chandra, et al., 1970; Elliott and La Valle, 1970] which itself is correlated with the plasmapause [Thomas and Andrews, 1968; Rycroft and Burnell, 1970]. Proton Coulomb losses should maximize inside the high density plasmasphere ($N \sim 10^3$ cm^{-3}), rather than the lower density ($N \sim$ 100-300 cm^3) plasmapause gradient region; hence Cole's heating process would not necessarily exhibit

plasmapause localization. Finally, Cornwall, Coroniti, and Thorne [1970; herein referred to as CCT] have argued that ring current protons dissipate most of their energy into ion cyclotron wave turbulence and the concomitant proton precipitation loss. This turbulent proton removal is most effective in regions of low Alfvén speed. For 10 to 50 KeV proton energies CCT have argued that the low densities found just outside the plasmapause provide a region of ring current stability. In sharp contrast, the high density plasmasphere and the low magnetic field region for $L \geq 5$ to 6 should be highly unstable. The proton ring current is thus spatially bounded by two regions of instability, which we tentatively associate with the ionospheric SAR-arc and proton auroral emissions. We finally note that within the plasmasphere the rapid proton energy transfer to ion cyclotron waves and energy loss via precipitation severely limits the amount of available energy that protons can dissipate by Coulomb collisions.

Before proceeding with our alternative description of the SAR-arc energy source, we briefly summarize the salient observational features of the arcs; a more complete discussion can be found in Roach and Roach [1963], Cole [1965], Nagy, et al., [1970].

a. Intensity: SAR-arc intensities range from hundreds of Rayleighs (R) to several KR. Higher intensities generally occur for large D_{st} [Rees and Akasofu, 1963], although the correlation exhibits considerable scatter [Nagy, et al., 1970].

b. Spectral Properties: The dominant oxygen line emission at 6300 A is accompanied by at most one or two per cent of 5577 A and insignificant amounts of 3914 A and H_β. Cole [1965] has convincingly argued that the SAR arc spectral purity suggests excitation by electrons with energies less

than a few electron volts, rather than by direct energetic particle bombardment.

c. Temperatures: Norton and Findlay [1969] and Chandra, et al. [1970] report electron temperatures of 4000-5000°K (0.4-0.5 eV) at altitudes between 900 and 2000 Km above a SAR-arc. Neutral temperatures are much colder ($\sim$ 1000°K), and remain essentially unchanged from inside to outside an arc [Roble, Hays, and Nagy, 1970a]. Ion temperatures are expected to equal neutral temperatures at SAR-arc heights, and to increase toward electron temperatures at high altitudes; Chandra et al. [1970] report ion temperatures of $\sim$ 4000°K at 900 km.

d. Spatial Location: SAR arcs occur between altitudes of 300 and 700 km with peak intensity near 400 km [Roach and Roach, 1963]. Their north-south extent is several hundred kilometers but they often extend for thousands of kilometers in longitude and may completely encircle the earth [Roach et al., 1962]. SAR-arcs also exhibit the local time asymmetry of the plasmapause [Glass et al., 1970] and occur on field lines which lie just inside the plasmapause, where the equatorial electron density is several hundred cm^{-3} [Chappell et al., 1970].

e. Temporal Morphology: SAR-arcs are observed during the rapid recovery phase of magnetic storms, some 10 to 20 hours after the main phase decrease begins. Their intensity is remarkably constant for periods of over 10 hours.

In the CCT ring current proton-magnetic storm model, the rapid recovery phase is controlled by the outward expansion of the plasmapause from the position of maximum storm-time compression. Recovery phase commences after the last major injection of protons into the inner magnetosphere; at this juncture of the storm, the ring current has attained maximum intensity and is

approximately symmetric in local time [Akasofu, 1969]. The plasmapause then expands outward into the symmetric ring current. Once inside the region of high plasma density, the ring protons become unstable generating intense ion cyclotron turbulence which results in their precipitation into the atmosphere (see Figure 1). This outward moving zone of turbulence encompasses a large fraction of the ring current, out to perhaps 5 Re, in about one half to one day.

In this paper we postulate that the intense ring current generated ion cyclotron wave turbulence is an important SAR-arc electron heat source. The wave energy is absorbed by thermal electrons on field lines near the plasmapause. In the inhomogeneous geomagnetic field, ion cyclotron wave ray tracing calculations by Kitamura and Jacobs [1968] have demonstrated that the wave normal rapidly rotates to large angles with respect to the magnetic field direction. Very oblique ion cyclotron waves inside the plasmapause have resonant Landau damping interactions [Kennel and Wong, 1967] with thermal plasmaspheric electrons (CCT). We therefore propose the following model of proton energy transport: protons just inside the plasmapause relinquish energy to ion cyclotron waves and are precipitated; the ion cyclotron waves are then Landau absorbed by thermal electrons; the resultant heat input into electrons is thermally conducted to the ionosphere to excite SAR-arcs on lines of force connected to the plasmapause. In this model ion cyclotron waves act as an intermediary which couples ring current proton energy to thermal electrons. We find that proton Coulomb dissipation is still important for warming plasmaspheric electrons to temperatures at which electron Landau damping becomes efficient.

In the above model the SAR-arc is localized just inside the position of the expanding plasmapause, and has a duration on the order of one half to one day. Furthermore, the symmetry of the recovery phase ring current implies that SAR-arcs are created at all local times, but with the local time vs. L value asymmetry of the plasmapause [Carpenter, 1966; 1970]. CCT have also argued that protons can only penetrate to distances of about 1/2 Re into the plasmasphere before being precipitated; this is consistent with the ring current observations of Frank [1967; 1970] (see also Russell and Thorne, 1970). Since the group velocity of ion cyclotron waves is almost parallel to the magnetic field, the region of the ion cyclotron turbulence, and hence electron Landau heating, will extend for only about 1/2 Re just inside the plasmapause. Therefore, the electron heat conduction to the ionosphere and the resulting SAR-arc excitation are limited to a narrow latitude range corresponding to field lines passing just inside the plasmapause.

With the spatial and temporal SAR-arc properties reasonably well determined, we turn to quantitative evaluation of ion cyclotron wave Landau electron heating. Section 2.0 reviews the ring current energy requirements, Cole's [1965] electron heating conduction theory, and evaluates the proton Coulomb dissipation rate for Frank's [1967] ring current spectrum. Section 3.0 briefly discusses the ion cyclotron turbulence theory for an average 100 gamma D_{st} magnetic storm. We argue that about 1/2 of the ring current proton energy is converted into ion cyclotron turbulence. We then estimate the wave energy flux and find it sufficient for SAR-arc production.

Section 4.0 considers electron Landau damping of ion cyclotron waves. We first perform ray tracing calculations at L = 3 using both diffusive equilibrium and gyrofrequency density models. We then compute the Landau

damping decrement following a ray path and hence determine the path integrated wave absorption. The calculations are performed for various wave frequencies and electron temperatures. For electron temperatures of one to several eV, electron Landau damping efficiently absorbs ion cyclotron wave energy and hence provides a sufficient heat source for SAR-arcs.

Section 5.0 describes a unified model for SAR-arc formation. We determine the total electron heat flux, resulting from both proton Coulomb losses and Landau absorbtion, as a function of electron temperature and the critical proton anisotropy for ion cyclotron instability. The computed electron heat flux is also converted to SAR-arc intensity using the results of Roble [1969]. By estimating the electron heat conduction losses, we then determine the equilibrium magnetospheric electron temperature and SAR-arc intensity. Section 6.0 summarizes and comments on the results.

2.0 REVIEW OF HOT ELECTRON THEORY OF RED ARCS

In Section 2.1 we evaluate the total ring current energy density for a magnetic storm of sufficient strength to produce a SAR-arc. Assuming a proton energy dissipation rate consistent with the plasmapause expansion or the SAR-arc duration, we estimate the fraction of ring current energy required to drive a SAR-arc. We then review Cole's [1965] electron heat conduction theory and determine the equatorial electron temperature necessary to sustain a red arc (Section 2.2). Using the proton energy spectrum measured by Frank [1967] and by Frank and Owens [1970], the Coulomb collisional transfer rate of proton energy to thermal electrons is then reevaluated (Section 2.3).

2.1 Ring Current Energy and Dissipation Time Scales

The ring current proton energy spectrum and energy density have been measured by Frank [1967] for the moderate magnetic storm of July 9, 1966, for which D_{st} was 50 gammas. Frank also showed that the total energy content of ring current protons agreed well with the Sckopke [1966] relationship. The data [after Frank and Owens, 1970] are summarized in Table I. Note that protons with less than 1.8 keV constitute only 2% of the total ring current energy. From the D_{st} SAR-arc correlation studies of Rees and Akasofu [1963], the July 9, 1966, magnetic storm was probably too small to produce an observable red arc. In order to estimate the ring current energy available under conditions when a SAR-arc might be produced, we assume that the proton energy spectrum observed by Frank [1967] remains unchanged, and hence that D_{st} is proportional to the proton number density. A 1 KR SAR-arc requires a storm $D_{st} \simeq 100$ gammas [Rees and Akasofu, 1963], and Table I indicates that the proton energy density would then be $\sim 5.4 \times 10^{-7}$ ergs cm^{-3}.

The total energy contained above an area of one cm^2 in the ionosphere at $L = 3$ can be obtained by multiplying the equatorial energy density by 5×10^{10} cm (50 for the contraction of the flux tube area, 10^9 cm for an effective length). Thus a storm with $D_{st} = 100$ gamma should have a total proton energy $W_+ = 3 \times 10^4$ ergs cm^{-2} available.

During the storm recovery CCT have noted that the total energy dissipation time scale t_+ is determined by the rate of the plasmapause expansion into the symmetric ring current; $t_+ \sim (0.5 - 1) \times 10^5$ sec. Alternatively, a similar value of t_+ could be determined from the rapid recovery phase [Akasofu, 1969] or the SAR-arc duration time scales. Notice that t_+ is much longer than a proton turbulent lifetime since only a small portion of the ring current is unstable at a given time. We may assume that a fraction f of the proton energy is dissipated into electron thermal energy to obtain the resultant electron heat flux available for red arc formation $fW_+t_+^{-1}$. Setting $fW_+t_+^{-1} = F \simeq 7 \times 10^{-2}$ ergs cm^{-2} - sec^{-1}, which is the required electron heat flux for a SAR-arc of about 1 KR intensity [Walker and Rees, 1968; Roble, 1969], and substituting for W_+ and t_+, we find $f \sim 0.25$.

In Figure 2 we synthesize the results of Walker and Rees [1968] and of Rees and Akasofu [1963] using the above estimates for f and t_+. We first equate the heat flux F to $fW_+t_+^{-1}$; W_+ is then converted to D_{st} using $W_+ = 3 \times 10^4 (D_{st}/100)$ so that we have $F = (f/t_+) 3 \times 10^4 (D_{st}/100)$. The calculated heat flux against SAR-arc intensity curves of Walker and Rees are then converted to D_{st} vs. SAR-arc intensity using the above relation with $f = 0.25$ and $t_+ = 0.5 \times 10^5$ and 10^5 seconds, thus giving the two theoretical curves shown in Figure 2. The measured D_{st} vs. intensity points from

Rees and Akasofu are also plotted in Figure 2 (error bars have been omitted for clarity). The two theoretical curves roughly bracket the measured points thus substantiating the estimated values of f and t_+ for a large range of red arc intensities and magnetic storm strengths. Hence for SAR-arc production, about one quarter of ring current proton energy must be transferred as heat to electrons; the time scale for the energy transfer is on the order of $0.5 - 1.0 \times 10^5$ seconds.

2.2 Equatorial Electron Temperature Required for SAR-Arc

Following Cole [1965], we assume that the equatorial electron temperature T_E is controlled by a balance between ring current proton dissipation and heat losses along the line of force to the ionosphere. Electron heat then flows from the equator to the ionosphere along lines of force and collisionally excites the SAR-arc. If the electrons inside the plasmasphere are collisional, the electron temperature T distribution along the magnetic field obeys the source and sink-free heat conduction equation

$$\frac{1}{a(S)} \frac{\partial}{\partial S} \left(a(S) \, K \frac{\partial T}{\partial S} \right) = 0 \qquad (2.1)$$

S is the length along a field line, $a(S) = B_I/B(S)$ is the flux tube area normalized to unity at the ionosphere where $B(S) = B_I$, and $K = 1.64 \times 10^{49} \, T^{5/2} \, cm^{-1} \, sec^{-1}$ is the parallel collisional thermal conductivity [Spitzer, 1962]. We solve (2.1) with the boundary condition that the heat flux at the ionosphere equal F :

$$K \frac{\partial T}{\partial S} \bigg|_I = F \qquad (2.2)$$

With (2.2), a double integration of (2.1) yields

$$T_E^{7/2} = T_I^{7/2} + \frac{7F}{2(1.64 \times 10^{49})} \int_{S_I}^{S_E} \frac{dS'}{a(S')} \quad . \tag{2.3}$$

If the ionospheric electrons are cold, $T_I < 1/2\ T_E$, T_I in (2.3) can be neglected, and we then can solve for the equatorial temperature T_E in terms of the ionospheric heat flux:

$$T_E = 2.86 \times 10^{-12}\ F^{2/7} \quad \text{(ergs)} \quad . \tag{2.4}$$

For a 1 KR SAR-arc, $F \simeq 7 \times 10^{-2}$ ergs/cm^2-sec, and $T_E \sim 1.3 \times 10^{-12}$ ergs. Thus the electron heat source required for red arc production must be capable of maintaining the equatorial electron temperature at about 1 eV.

We note, as has Cole [1965], that the heat conduction relation (2.1) is valid only when the Coulomb electron-electron collision time is less than the electron bounce time. The collision time is $t_C \sim 1.3 \times 10^5\ N^{-1}\ T^{3/2}$ [Spitzer, 1962] where N is the density and T the electron energy in eV; the bounce time at L = 3 is approximately $t_B \sim 1.2 \times 10^2\ T^{-1/2}$. For $T \sim 1$ eV, $t_B \simeq t_C$ at $N \simeq 10^3$ cm^{-3}, a typical plasmaspheric density.

From CCT, however, ring current protons destabilize ion cyclotron waves and are precipitated along the plasmapause where $N \sim 200\text{-}300$ cm^{-3}; hence few protons, especially during recovery phase, penetrate the plasmasphere to regions of 10^3 cm^{-3} density. Assuming that electron heating occurs where the ring current overlaps the plasmapause, we find for $T \sim 1$ eV and $N \sim 300$ cm^{-3} that $t_C = 4\ t_B$. The electrons are approximately collisionless and thus remain quasi-trapped in earth's magnetic mirror field. Nevertheless,

pitch angle isotropy is approximately maintained across the loss cone by collisions as in the case of strong turbulent pitch angle diffusion discussed by Kennel [1969]. Heat conduction to the ionosphere then occurs by precipitation. Since the electron thermal flux $J = N(T/M_-)^{1/2}$ is approximately isotropic, the precipitation electron heat flux can be estimated as

$$F = JT \approx \frac{NT^{3/2}}{\sqrt{M_-}} \quad . \tag{2.5}$$

Note that in strong diffusion, heat conduction varies as $T^{3/2}$, a much weaker dependence than the $T^{7/2}$ variation of collisional heat conduction. For a 1 KR SAR-arc with $F \simeq 0.07$ ergs cm^{-2} sec^{-1} and $N \simeq 300$, equation (2.5) yields $T_E \simeq 2.2$ eV for the equatorial electron temperature.

Near the ionospheric SAR-arc region, precipitating electrons again become collision dominated. Hence gradients of electron temperature should be seen in the topside ionosphere above red arcs [Roble, et al., 1970b].

2.3 Ring Current Proton Coulomb Energy Loss Rate

In Cole's [1965] theory the heat source for magnetospheric electrons is the loss of proton energy by Coulomb collisions. Here we reestimate the Coulomb heating rate averaged over the observed ring current proton energy spectrum [Frank, 1967] for a plasmapause density of $\simeq 300$ cm^{-3}. A proton of energy E_+ moving in a thermal electron gas loses energy at a rate given by [Spitzer, 1962]

$$\frac{\partial E_+}{\partial t} = - \frac{E_+}{T_c(E_+)}$$

where

$$T_c(E_+) = \frac{2.5 \times 10^6 \, E_+^{1/2}}{N \, G} \qquad (2.6)$$

E_+ is measured in keV and G is a dimensionless function of the ratio of mean proton to electron velocity. When this ratio is large, as it is for 20 KeV protons and electrons of less than a few eV, $T_c(E_+)$ is essentially independent of electron temperature.

The mean time T_c for Coulomb dissipation is found by averaging (2.6) over the ring current energy spectrum given in Table I and substituting $N = 300$ cm^{-3}. We find $T_c \simeq 10^6$ sec, which is about 30 times longer than the dissipation time quoted by Cole for $N = 100$ cm^{-3} and an average proton energy of 1 KeV. For a storm strength with $D_{st} = 100$ gammas ($W_+ = 3 \times 10^4$ ergs/cm^2) the heat flux to electrons from proton Coulomb collisions is $W_+/T_c = 0.03$ ergs cm^{-2} sec^{-1}, which according to Walker and Rees [1968] would produce about 100 R in a SAR arc.

Although inadequate as the sole electron heat source for SAR arcs, a proton Coulomb dissipation rate of 0.03 ergs cm^{-2} sec^{-1} can raise the electron temperature to about 0.6 eV [from (2.4)] or 1.3 eV [from (2.5)], depending on the heat conduction law. We show in section 4.0 that electron temperatures on the order of 1 eV are required before Landau damping of ion cyclotron waves becomes effective. Hence proton Coulomb heating of electrons is important as a primer for Landau damping.

3.0 Energy in Ion Cyclotron Turbulence

After cessation of strong convection and ring current injection, upward ambipolar diffusion of ionospheric plasma and corotation of the bulge region

[Carpenter, 1970; Chappell, et al., 1970a] gradually repopulates the plasmasphere or corotation zone. For a uniform ionospheric filling rate, the smaller volume of low L-shell flux tubes results in an effective plasmapause outward expansion. Thus symmetric ring current protons are, in effect, transported across the plasmapause and are thereby able to generate intense ion cyclotron wave turbulence. (Of course additional proton transport by radial diffusion cannot be discounted.) Since SAR arcs are observed between $L \sim 2$ and 4, we evaluate theoretical parameters at the mean location $L = 3$. In this section we reformulate for $L = 3$ and $D_{st} = 100$ gammas, the estimates of CCT for the ion cyclotron growth rate γ_{cyc}, the fraction of proton energy lost to ion cyclotron waves, and the turbulent wave intensity. Section 4.0 considers the Landau absorption of ion cyclotron waves by plasmaspheric electrons.

Instability of ion cyclotron waves with frequency ω requires that the proton distribution function have a pitch angle anisotropy $A^+ > A_c$ where

$$A_c = x/(1-x) \quad . \tag{3.1}$$

Here $x = \omega/\Omega_+$, where Ω_+ is the ion gyrofrequency. A^+ has been defined by Kennel and Petschek [1966] and by Cornwall [1966] as a velocity space integral of gradients in the proton distribution function f^+. As an example, if $f^+ \sim \sin^{2n}\alpha$, where α is the proton pitch angle, then $A^+ \equiv n$. By using the cyclotron resonance condition $\omega - k_{\parallel} v_{\parallel} = -\Omega_+$ and the ion cyclotron wave dispersion relationship, we find that for a given anisotropy A^+, only protons whose parallel energy $M_+ v_{\parallel}^2/2$ exceeds

$$E_R = E_M/[A^{+2}(1 + A^+)] \qquad (3.2)$$

can partake in the instability. Here E_M is the magnetic energy per particle, $E_M = B^2/8\pi N \simeq 2.2 \times 10^3\ N^{-1}$ KeV at $L = 3$. The growth rate for waves propagating parallel to the magnetic field is [Kennel and Petschek, 1966]

$$\gamma_{cyc} = \frac{\pi}{2}\ \frac{\Omega_+}{x}\ \frac{(1-x)^2}{1 - x/2}\ \eta(A^+ - A_c) \qquad . \qquad (3.3)$$

where η is the fraction of protons with parallel energy greater than E_R.

Now consider a magnetic storm with $D_{st} = 100$ gammas. Since the time scale for density accumulation in the expanding plasmapause is reasonably slow, we note from (3.2) that the highest energy ring current protons should become unstable first; lower energy protons enter unstable cyclotron resonance at higher densities. For a given average proton pitch angle anisotropy A^+, the instantaneous ion cyclotron wave spectrum should thus be dominated by the higher unstable frequencies near the upper limit $\omega/\Omega_+ \simeq A^+/1+A^+$. Typical anisotropies might range from $A^+ \sim 1/2$ to 3, with the higher values occurring during the most intense storms and at low L-shells. Thus near the magnetic equator ω/Ω_+ is expected to be between 1/3 and 3/4.

From (3.2) ring current protons with 10 to 50 KeV energies require densities on the order of 100 cm^{-3} or more for unstable ion cyclotron interactions; to ensure instability we choose $N = 300\ cm^{-3}$ in what follows. From Table I, the ring current proton density appropriate for $D_{st} = 100$ gammas is about 20 cm^{-3} [Frank and Owens, 1970], so we have $\eta = 20/300$. For $\Omega_+ = 100$ rad sec^{-1}, and $A^+ - A_c \simeq 1/4$, the ion cyclotron growth rate is $\gamma_{cyc} \simeq 4\ sec^{-1}$. When path integrated, such large growth rates ensure intense ion cyclotron turbulent wave amplitudes [Cocke and Cornwall, 1967; CCT].

Ion cyclotron wave energy is obtained at the expense of proton perpendicular kinetic energy. Protons diffuse in velocity space along the characteristic curve [Gendrin, 1968; Haerendel, 1970; Eather and Carovillano, 1970]

$$v_\perp^2 + [v_\parallel - (\omega/k_\parallel)]^2 + v_A^2 \log x = \text{const.} \tag{3.4}$$

where v_A is the Alfvén speed, $\omega/k_\parallel$ is the parallel ion cyclotron phase speed given approximately by

$$\omega/k_\parallel = v_A(1-x)^{1/2} \tag{3.5}$$

and $v_\parallel$ is related to x by the resonance condition

$$\frac{v_\parallel}{v_A} = -\frac{1}{x}(1-x)^2 \tag{3.6}$$

From (3.4) - (3.6), we find that the predominance of high frequencies in the turbulent wave spectrum implies that a ring current proton which diffuses from flat pitch angles to the loss cone relinquishes an energy $1\text{-}2E_M$ or some 10 to 20 KeV. Hence approximately 1/2 of the ring current energy is transferred into ion cyclotron waves. Recall that the fraction of ring current energy needed for a red arc is $f \simeq 0.25$.

We now estimate the ion cyclotron turbulent wave amplitude. From CCT, ion cyclotron turbulence should exist for a region of about 1/2 R_e inside the plasmapause. During the plasmapause expansion over 1/2 R_e, the proton flux will be rapidly reduced to the stably trapped limit. Hence the maximum proton precipitation lifetime must be governed by the time of plasmapause expansion

across 1/2 R_e . If we estimate the expansion velocity as the total distance the plasmapause moves during recovery phase, $\simeq 3\ R_e$, divided by $t_+ \simeq 0.5\text{-}1.0 \times 10^5$ seconds, we find $v \simeq 3 \times 10^4$ cm sec^{-1} . The maximum precipitation lifetime is then $t_L \simeq 10^4$ seconds. We can now estimate the pitch angle diffusion coefficient during recovery phase as [Kennel and Petschek, 1966; Cornwall, 1966]

$$D \simeq \frac{1}{t_L} = \Omega_+ \left(\frac{B'}{B_o} \right)^2 \frac{t_{int}}{t_B} \tag{3.7}$$

where B' is the wide band r.m.s. turbulent wave amplitude, and t_{int}/t_B is the fractional time a proton spends in the ion cyclotron turbulent region; for L = 3, $t_{int}/t_B \sim 1/5$. For $\Omega_+ = 100$ rad/sec and $t_L = 10^4$ seconds, (3.7) yields $B' = 2$ gammas.

The energy flux in ion cyclotron waves is

$$F_{wave} = \frac{(B')^2}{8\pi} V_A \tag{3.8}$$

For $L = 3$ and $N = 300$ cm^{-3} , $V_A \simeq 2 \times 10^8$ cm sec^{-1} and (3.8) yields $F_{wave} \simeq 3 \times 10^{-3}$ ergs cm^{-2} sec^{-1} , which corresponds to a wave energy flux at the ionosphere of 0.15 ergs cm^{-2} sec^{-1} or approximately twice the energy flux needed to produce a 1 KR red arc. Therefore, if the turbulent ion cyclotron wave energy could efficiently be converted into electron thermal energy, the resultant electron heat flux would be sufficient to sustain a SAR arc appropriate for a 100 D_{st} storm. Furthermore since the ion cyclotron turbulence is localized to a narrow region just inside the plasmapause, and since the wave group velocity is essentially guided along the magnetic field, the red arc would exhibit a corresponding spatial localization in the ionosphere.

In the next section we demonstrate that electron Landau absorption of ion cyclotron waves completes the coupling between the loss of ring current proton energy and the heating of plasmaspheric electrons to the required SAR-arc temperatures of several eV.

4.0 ELECTRON LANDAU ABSORPTION OF ION CYCLOTRON WAVES

The absence of definitive ground micropulsation detection of the large ion cyclotron wave amplitudes near the plasmapause immediately suggests that part of the wave energy might be absorbed in the plasmasphere. We notice at once that the ion cyclotron phase velocity, essentially the Alfvén speed, is comparable to the thermal velocity of plasmaspheric electrons. This suggests that Landau damping may be important. (Low energy protons, of a few KeV, have similar velocities, but are of much lower density than electrons and hence are relatively unimportant.) Ray tracing calculations by Kitamura and Jacobs [1968] have demonstrated that the wave normal angle of ion cyclotron waves propagating in the anisotropic magnetosphere rapidly rotates to large angles with respect to the magnetic field direction. Oblique ion cyclotron waves can then experience appreciable Landau resonant energy exchange with thermal electrons [Kennel and Wong, 1967]. Although the resonant interaction increases only the parallel energy of the electrons, non-resonant processes such as collisions distribute the thermal energy and maintain approximate pitch angle isotropy. This section evaluates the total path integrated Landau absorption of ion cyclotron wave energy for a variety of electron temperatures and wave frequencies. Section 5.0 then estimates the combined electron heat flux from proton Coulomb dissipation and Landau damping, and determines the resulting SAR-arc intensity.

The local Landau damping decrement $|\gamma_L|$ for ion cyclotron waves propagating through a Maxwellian electron plasma is derived in the Appendix [equation (A.17)]

$$\frac{|\gamma_L|}{\omega} = \frac{1}{\sqrt{\pi}} \left[\frac{\tan\theta}{\tan\theta_{res}} \right]^2 \left(\frac{v_{ph}}{v_{th}} \right)^3 \exp[-(v_{ph}/v_{th})^2] \qquad (4.1)$$

θ is the angle between the wave propagation vector and the ambient magnetic field; $\theta_{res} = \arctan [(\Omega_+\Omega_-)^{1/2}/\omega]$ is the resonant wave normal angle at which the wave phase velocity v_{ph} is zero and $v_{th} = [2T/M_-]^{1/2}$ is the electron thermal speed.

Clearly $|\gamma_L|$ is a very sensitive function of the four parameters θ, θ_{res}, v_{ph}, and v_{th}. Since our goal is to determine the total path integrated absorption, it is mandatory that these parameters be known precisely along a ray path. The calculations were therefore performed using the Stanford ray tracing program to follow representative ion cyclotron waves propagating through a model magnetosphere. A dipole magnetic field at L = 3 was adopted; hence self-consistent ring current distortions of the magnetic topology near the equatorial plane are neglected. Two density models are used: a) diffusive equilibrium, which is probably most representative of the quiet time plasmasphere; b) the gyrofrequency model, N/B = constant, which is more appropriate for collisionless plasma conditions encountered during the plasmasphere repopulation when large density gradients along the field are possible. The actual density distribution near the expanding plasmapause probably resides between these two extremes.

The selection of initial conditions for the ray tracing calculations is, of course, somewhat arbitrary. Ion cyclotron unstable growth probably occurs for a latitude range of order ± 20° about the equator. In addition a large range of wave normal angles are likely to be unstable [Kennel and Wong, 1967; Dobês, 1970]. Clearly, the fate of every wavelet in the turbulent wave spectrum cannot be determined. Therefore we choose to follow test waves which start at

a latitude of -20° with propagation vectors parallel to the ambient field and then propagate across the equatorial plane towards the ionosphere. These waves spend a maximum time in the unstable growth region, and hence might be expected to dominate the wave spectrum. We can thus at best determine a representative electron Landau absorption rate.

The Landau damping decrement was evaluated at small latitude intervals along the ray path, and then integrated to obtain the total residual wave energy $\exp[-\int 2\,|\gamma_L|\,dt]$ or the total electron absorption coefficient $a = 1 - \exp[-\int 2\,|\gamma_L|\,dt]$. As an example, in Figure 3 the instantaneous Landau damping rate $|\gamma_L|$ for waves with $\omega/\Omega_+ = 2/3$ at the equator is plotted against latitude; recall that ion cyclotron instability at the equator requires $A^+ \sim 2$ for $\omega/\Omega_+ = 2/3$. The electron temperature of 2 eV is typical of SAR-arc conditions (see sections 2.0 and 5.0) and the equatorial electron density $N = 300\ cm^{-3}$ is appropriate for the expanding plasmapause (see section 3.0). $|\gamma_L|$ remains small for the first 20° of propagation, thus ensuring a large region of uninhibited ion cyclotron unstable growth; it then peaks strongly near 15° - 20° latitude. $|\gamma_L|$ rises due to the increase in the wave normal angle θ which reaches about 80 to 85° near the peak; note that $\theta \sim 60°$ at the equator. The rapid decrease in $|\gamma_L|$ at high latitudes is due to the increase of the Alfvén velocity which from (4.1) exponentially reduces $|\gamma_L|$ when $v_A >> v_{th}$. Both density models yield similar damping decrements although the N/B = constant model has a slightly broader region of wave damping. Since the density models differ appreciably only at high latitudes, where $|\gamma_L| \to 0$ anyway, the calculation is expected to be reasonably insensitive to the actual density distribution. The path integrated damping decrement for this case was $\int 2|\gamma_L|dt \sim 2$, so that approximately 80% of the wave energy is absorbed by plasmaspheric electrons.

In Figure 4 the residual wave energy $(B'_{final})^2/(B'_{initial})^2 = \exp[-\int 2|\gamma_L|dt] = 1-a(T)$ is plotted against plasmaspheric electron temperature using the wave frequency ω/Ω_+ or critical anisotropy A^+ as a parameter. Again an equatorial density $N = 300\ cm^{-3}$ at $L = 3$ was used. At low temperatures little Landau damping occurs since very few electrons are in Landau resonance with ion cyclotron waves. At temperatures above a few eV Landau absorption essentially saturates. Again note the relative insensitivity of the calculations to the model of electron density distribution. From Figure 4 we conclude that under typical storm and recovery phase conditions when $A^+ \geq 1$, a sizable fraction of the ion cyclotron wave energy will be Landau absorbed by thermal plasmaspheric electrons.

By starting waves at -20° latitude, the above ray tracing computations are weighted in favor of attaining large wave normal angles and consequently large Landau damping decrements. Calculations have shown that waves starting parallel to the magnetic field at the equator reach wave normal angles of only about 60°, near the peak in $|\gamma_L|$, and hence are only weakly Landau damped. On the other hand, such waves originating at the equator experience less unstable growth than waves starting at -20° latitude and, due to the exponential nature of wave growth, should have considerably smaller amplitudes. However, since we have not solved for the ion cyclotron unstable wave spectrum, our calculations are at best an approximate estimate of the overall electron Landau absorption of ion cyclotron turbulence.

Finally, since the group velocity of ion cyclotron waves is essentially guided along the magnetic field (a result which is confirmed by all ray tracing computations performed here), the wave energy is absorbed by electrons in a small region approximately 1/2 R_e wide just within the plasmapause. The

next section considers the resultant electron heat flux arising from wave Landau damping and proposes a unified theory for SAR-arc formation localized to the plasmapause.

5.0 TOTAL ELECTRON HEAT FLUX AND RESULTING SAR-ARCS INTENSITIES

In the previous sections the multiple links in the energy transport chain were evaluated for a main phase storm of D_{st} = 100 gammas. We now estimate the total electron heat flux incident on the ionosphere and use the conduction models of Section 2.2 to determine the equilibrium equatorial electron temperature and SAR-arc intensity.

The electron heating rate from Landau absorption of ion cyclotron turbulence is approximately given by

$$F_L = a(T)\, F_{wave} \tag{5.1}$$

where $a(t) = 1 - \exp[-\int 2|\gamma_L|dt]$ is the absorption coefficient. In section 3.0 we estimated the turbulent r.m.s. wave amplitude as $B' = 2$ gammas and the wave energy flux as $F_{wave} \simeq 0.15$ ergs cm^{-2} sec^{-1}. Since some waves may never attain large wave normal angles and are consequently not Landau damped, we compensate for this loss by taking $F_{wave} = 0.1$ ergs cm^{-2} sec^{-1} in what follows.

Electrons are also heated by proton Coulomb dissipation. Since ring current protons are lost before they can penetrate 1/2 R_e into the plasmasphere [CCT], the Coulomb dissipation will also be confined to a narrow region just inside the plasmapause. Therefore to obtain the total electron heating rate F_{tot} we add the proton Coulomb heating derived in section 2.3, $W_+/T_c \simeq 0.03$ ergs cm^{-2} sec^{-1} for $D_{st} = 100$ gammas, to F_L to obtain

$$F_{tot} = a(T)\, F_{wave} + (W_+/T_c) \tag{5.2}$$

or

$$F_{tot} = 0.1\ a(T) + 0.03\ (\text{ergs cm}^{-2}\ \text{sec}^{-1}) \quad . \tag{5.3}$$

In Figure 5 the ray path calculations of $a(T)$, from section 4.0, are used to plot F_{tot} against electron temperature T_E for several proton anisotropies A^+ (or alternatively unstable wave frequencies $\omega/\Omega_+ = A^+/1+A^+$). We have also plotted the collisionless strong diffusion heat conduction law (2.5) and included for comparison the collisional heat conduction law (2.4). On the right hand side of Figure 5 we have converted the total electron heat flux to SAR-arc intensity using the results of Walker and Rees [1968] and Roble [1969].

The equilibrium electron temperature and electron heat flux incident upon the ionosphere is given by the intersection of F_{tot} with the strong diffusion heat conduction curve; at this point the electron heating rate is balanced by heat conduction losses. Thus for $A^+ = 1$, $T_E = 2.0$ eV and $F_{tot} = 0.06$ ergs cm^{-2} sec^{-1}; the corresponding SAR-arc intensity is about 800 R. At larger proton anisotropies, the wave spectrum is dominated by higher frequency ion cyclotron waves which are subject to stronger electron Landau absorption. This results in a higher electron temperature, larger electron heat flux, and a more intense SAR-arc. Hence the ring current proton-ion cyclotron wave-electron Landau absorption model when combined with proton Coulomb dissipation can provide a sufficient electron heat flux to the ionosphere to excite the observed SAR-arc intensities.

So far only the equilibrium state has been discussed. The temporal evolution of the electron temperature from cold plasmaspheric values of perhaps as low as 0.2 eV to SAR-arc values is undetermined. Although we do not

explicitly solve for it, the temporal development of the electron temperature can be qualitatively obtained from Figure 5. Suppose initially that $T_E \leq 0.6$ eV. Then, as soon as the ring current overlaps the plasmapause, proton Coulomb dissipation starts electron heating. Landau absorption contributes negligibly unless $A^+ \sim 2$ to 3. The electron temperature rises since heat conduction losses are less than heat input. By the time $T_E \sim 0.6$ eV, electron Landau absorption of ion cyclotron turbulence has begun to contribute to the total heat flux F_{tot}. The energy flux and electron temperature continue to increase until the heating rate is balanced by strong diffusion heat conduction to the ionosphere. Thus, although capable of sustaining only about a 100 R SAR-arc, proton Coulomb dissipation is important for raising the electron temperature to values at which electron Landau absorption becomes efficient. Of course, during main phase, there may be other processes acting in conjunction with Coulomb dissipation to heat the electrons to this critical temperature.

The numerical estimates in Figure 5 are based on specific values of various magnetospheric parameters: $D_{st} = 100$ gammas, $L = 3$, $N = 300$ cm^{-3}, and $B' = 2$ gammas. Clearly, the sensitivity of the equilibrium red arc intensity to plasmapause location and structure, proton anisotropy, and the ion cyclotron turbulent wave spectrum suggests that red arc intensities are not uniquely determined by D_{st} alone, and that for a given D_{st} value a wide range of arc intensities is possible. Since our theoretical estimates are rather imprecise, simultaneous measurements of all the above variables are needed to firmly establish the interrelations between the various parameters and red arc intensity.

6.0 DISCUSSION

6.1 Summary

Accepting Cole's [1964; 1965] original hypotheses that SAR arcs are excited by thermal electron heat conduction from the magnetosphere and that the ultimate arc energy source is the ring current, we have developed a model for the electron heat source which is consistent with recent ring current and SAR arc measurements. We summarize the salient features (see Figure 6).

a) During the rapid recovery phase of a magnetic storm, the plasmapause moves outward into the approximately symmetric ring current. When N reaches $\sim$ 100, ring current protons destabilize ion cyclotron waves and are precipitated; a narrow zone, 1/2 R_e wide, of ion cyclotron turbulence is formed just inside the expanding plasmapause.

b) Ring current protons dissipate about 1/2 their energy in ion cyclotron waves. A small fraction of the proton energy is dissipated in Coulomb collisions with thermal electrons. The remaining proton energy is lost as precipitation.

c) Obliquely propagating ion cyclotron waves have resonant Landau damping interactions with thermal plasmaspheric electrons. The rate of Landau absorption depends sensitively on total density, electron temperature, wave normal angle, and proton anisotropy.

d) Calculations of the total path integrated electron Landau absorption coefficient demonstrate that a significant fraction, approaching

unity for high electron temperatures and large proton anisotropies, of the ion cyclotron turbulent wave energy is converted into electron heat.

e) For a 100 gamma D_{st} storm the total electron heat flux provided by Landau absorption and proton Coulomb dissipation is sufficient to excite SAR-arcs with intensities of several 100 R's to a few KR's.

The above model predicts that:

f) SAR arcs should be localized to lines of force which lie just inside the plasmapause.

g) The north-south latitudinal extent of SAR-arcs should be several hundred kilometers.

h) SAR-arcs should occur at essentially all local times, with a latitude vs. local time dependence similar to that of the plasmapause. Hence at a given local time SAR-arcs should exhibit a general motion to higher latitudes as the rapid recovery phase progresses.

i) SAR-arcs should persist throughout the rapid recovery phase, or about one-half to one day. Red arcs intensities should greatly diminish after proton fluxes are reduced to the stably trapped limit; after this point only Coulomb dissipation remains but is weakened by the lower proton fluxes.

j) The SAR-arc intensity depends sensitively on the proton anisotropy; large anisotropies produce intense red arcs.

In the following sections we comment on several features of SAR-arcs not previously discussed.

6.2 Proton Precipitation Fluxes and SAR Arc Spectral Purity

The SAR arc spectrum consists predominantly of 6300 Å with very little spectral contamination from other auroral emissions; this spectral purity originally led Cole [1965] to the electron heat conduction excitation hypothesis. During rapid recovery phase, ring current protons inside the plasmapause precipitate [CCT] as well as heating electrons via ion cyclotron waves. We must therefore inquire about the magnitude of proton precipitation fluxes and the intensities of various auroral emission lines which might be directly excited by the energetic proton bombardment.

The ratio of the proton precipitation flux J_p to the trapped flux J_T is [Coroniti and Kennel, 1970]

$$J_p/J_T = t_{min}/t_L \quad . \tag{6.1}$$

$t_{min} = 2t_B/\alpha_o^2$ is the minimum precipitation lifetime [Kennel and Petschek, 1966]; α_o is the pitch angle of the equatorial loss cone. For ring current protons at L = 3, t_{min} = 1500 seconds. From section 3.0, we estimate $t_L \sim 10^4$ sec. Since the total trapped proton flux is of order $J_T \simeq 10^9$ cm^{-2} sec^{-1}, we expect $J_p \simeq 10^8$ cm^{-2} sec^{-1} along a narrow region just within the plasmapause during the storm recovery.

To determine the directly excited emission intensities, we must first recognize that these precipitation fluxes are not of the type commonly studied in works on proton auroras [Eather, 1967]; i.e., proton beams with very small pitch angles. Since t_{min}/t_L is reasonably small, precipitation is near the weak diffusion limit; hence the loss cone is practically empty, and protons which reach the ionosphere have very flat pitch angles. Second, the north-south

ionospheric spatial extent over which protons precipitate is about 300 Km or about the SAR arc thickness; thus precipitation is highly collimated. Between 400 and 1000 km altitude, the proton charge exchange mean free path is on the order of 200-300 km; hence all precipitating protons suffer several charge exchange collisions before reaching the 200 to 300 km altitude region where direct auroral excitation occurs. However, when an almost trapped proton with a very flat pitch angle charge exchanges, the resulting fast neutral hydrogen atom has a very high probability of leaving the collimated precipitation region before it suffers a further charge exchange. The probability of a fast neutral hydrogen returning to the precipitation region after having left it, and being reconverted to a proton, is negligible. Therefore, the collimated, flat pitch angled precipitating protons are spatially spread out by high altitude charge exchange interaction, so that the energetic proton flux reaching the emission region is greatly reduced from the incident precipitation flux at 1000 km altitude.

Without detailed calculations, a precise determination of the resulting proton flux at 200-300 km altitudes is difficult. However, since protons suffer at least 2 to 3 charge exchange collisions, and since the losses are practically irreversible, we estimate that the proton flux is degraded by a factor exp(-2) to exp(-3) or 10^{-1} to 0.5×10^{-1}. Hence the energetic proton flux available for direct auroral excitation should be about 5×10^{6} to 10^{7} cm^{-2} sec^{-1}.

The auroral emission to be expected from flat pitched 4 keV protons has been calculated by Prag et al. [1966]. The average energy of precipitated ring current protons might be around 15-20 keV (which is less than the average energy of trapped protons, because a proton loses a good fraction of its

energy as it diffuses toward the loss cone), so there is some uncertainty in extrapolating the above authors' results. Fortunately, most of the important charge-exchange and excitation cross sections vary by less than a factor of two from 4 to 15 keV. Hence, for a rough estimate we multiply the emission rates of Prag et al. by a factor of 5 and find that a flux of 10^7 cm^{-2} sec^{-1} protons should yield about 4 R of 3914 A, 8 R of 6300 A, 4-5 R of 5577 A, and 1.6 R of H_β (4860A). These values are still comfortably inside the experimental detection thresholds of some tens of Rayleighs. For comparison, Eather [1967] gives about 20 R of H_β for the same flux, with a full loss cone. Hence precipitating ring current protons do not greatly contaminate the spectral purity of SAR-arcs.

6.3 Main Phase

SAR-arcs occur primarily during recovery phase but not often during the main phase of a magnetic storm. Main phase is dominated by substorms, strong convection distortions of the plasmapause [Carpenter, 1970], and intense ring current proton injection, all with three hour or less repetition time scales. Therefore, although transient heating of plasmaspheric electrons by ion cyclotron waves, proton Coulomb collisions, or other processes, undoubtedly occurs during main phase, the repeated stripping away of the plasmapause by convection events [Chappell et al., 1970b] probably prevents the formation of the well collimated region of hot electrons needed for SAR-arc excitation. Thus SAR-arcs would not be expected during main phase even though intense ring current fluxes are present, but would occur during recovery phase when the plasmapause is reasonably quiescent.

6.4 Localization of SAR Arcs to $2 < L < 4$

SAR-arcs are rarely detected outside the region $2 \leq L \leq 4$. The lower L-shell limit corresponds to the innermost known penetration of the plasmapause [Carpenter, 1966] and, therefore, the ring current. On auroral lines of force $L > 5$ outside the plasmapause $E_M = B^2/8\pi N$ may be sufficiently small during storm condition ($N > 10$) that ion cyclotron waves are again destabilized by protons of ring current energies. Here ion cyclotron wave turbulence and proton precipitation are expected to occur over a broad spatial region, thus producing the proton aurorae [Eather, 1967; Eather and Carovillano, 1970]. Therefore during the rapid recovery phase the flux of ring current protons for $L > 5$ is reduced below the stably trapped limit. When the plasmapause has expanded out into the auroral region late in the rapid recovery phase, proton fluxes should have been reduced to a level where they are stable even inside the plasmapause; thus no SAR arcs would be expected.

6.5 Ground Detection of Ion Cyclotron Turbulence

Our model predicts intense ion cyclotron turbulence with amplitudes 1 - 2 gammas just inside the plasmapause; the expected wave frequencies at $L = 3$ are 5 to 10 Hz. Even if a sizable fraction of the ion cyclotron wave energy is not electron Landau damped and the waves consequently propagate to the lower ionosphere, ionospheric absorption below about 200 km probably prevents most of these waves from being detected on the ground. Hence a correlation between SAR-arcs and micropulsations would not necessarily be expected unless lower frequency, 1 Hz, waves are also generated by the high energy tail of the ring current protons or possibly by the Davis-Williamson [1963] protons.

APPENDIX

ELECTRON LANDAU DAMPING DECREMENT FOR ION CYCLOTRON WAVES

For a uniform, homogeneous plasma the electron Landau damping decrement for ion cyclotron waves derived by Kennel and Wong [1967] is

$$\frac{\gamma_L}{\omega} = \pi \frac{\omega_{p_-}^2}{\omega^2} \int_0^\infty v_\perp^3 \, dv_\perp \int_{-\infty}^\infty dv_\parallel \, \delta[v_\parallel - (\omega/k_\parallel)] \, \theta_o \frac{\partial F^-(v)}{\partial v_\parallel} \tag{A.1}$$

where

$$\theta_o = \frac{1}{\rho} \left| (R-L) \, J_1 \left(\frac{k_\perp v_\perp}{|\Omega_-|} \right) + 2M \frac{v_\parallel}{v_\perp} \, J_o \left(\frac{k_\perp v_\perp}{|\Omega_-|} \right) \right|^2 \tag{A.2}$$

$$\rho = (n^2-L)^2 \frac{\partial}{\partial \omega} (\omega R) + (n^2-R)^2 \frac{\partial}{\partial \omega} (\omega L) + 2M^2 \frac{\partial}{\partial \omega} (\omega P)$$

$$+ 2n^2 \left(\frac{P(n^2-S) \cos\theta}{P - n^2 \sin^2\theta} + D^2 \right) \tag{A.3}$$

$$M = \frac{n^2 \cos\theta \sin\theta \, (n^2-S)}{P - n^2 \sin^2\theta} \tag{A.4}$$

$$\left.\begin{matrix} R \\ L \end{matrix}\right\} = 1 - \sum_{+,-} \frac{\omega_{p_\pm}^2}{\omega(\omega \pm \Omega_\pm)} \tag{A.5}$$

$$P = 1 - \sum_{+,-} \omega_{p_\pm}^2 / \omega^2 \tag{A.6}$$

$$\left.\begin{matrix} S \\ D \end{matrix}\right\} = \frac{R \pm L}{2} \tag{A.7}$$

$$n^2 = k^2 c^2 / \omega^2 \tag{A.8}$$

$F(v)$ is the electron distribution function normalized so that $\int F(v)\, d^3v = 1$, and $v_{\parallel}$, $v_{\perp}$ are the electron velocities parallel and perpendicular to the ambient magnetic field of strength B. $\omega_{p_{\pm}} = (4\pi Ne^2/M_{\pm})^{1/2}$ are the proton (+) and electron (-) plasma frequencies and $\Omega_{\pm} = \pm eB/M_{\pm}c$ are the respective gyrofrequencies; N is the density, e the electronic charge, $M_{\pm}$ the particle mass, and c is the velocity of light. Gaussian units are used throughout. θ is the angle between the wave vector $\underset{\sim}{k}$ and the magnetic field, and $k_{\parallel}$, $k_{\perp}$ are the components of $\underset{\sim}{k}$ parallel and perpendicular to B. The Bessel functions J_o and J_1 in (A.2) give the damping contribution from the longitudinal and transverse electric field components, respectively. The Dirac-Plemelj delta function $\delta[v_{\parallel} - (\omega/k_{\parallel})]$ in (A.1) selects Landau electrons whose parallel velocity equals the wave parallel phase speed $\omega/k_{\parallel}$. For inhomogeneous magnetic fields (A.1) is valid if the radius of curvature greatly exceeds a typical wavelength.

We now simplify (A.1). First, terms of order $(\omega/\Omega_+)^2$ and higher are small and can be neglected. For ion cyclotron waves,

$$\frac{k_{\perp} v_{\perp}}{|\Omega_-|} = \frac{\omega}{|\Omega_-|} \tan\theta \frac{v_{\perp}}{v_{\parallel}} \sim \left(\frac{M_-}{M_+}\right)^{1/2} \left(\frac{\tan\theta}{\tan\theta_{res}}\right) << 1$$

where

$$\tan\theta_{res} = \frac{|\Omega_+\Omega_-|^{1/2}}{\omega} \tag{A.9}$$

gives the wave normal angle of the resonance cone at which the index of refraction $n \to \infty$. Hence in (A.2) J_o and J_1 can be expanded in the small argument limit. In (A.2) the longitudinal contribution (J_o term) dominates the transverse contribution (J_1 term) at large wave normal angles

by the fraction $2 \tan^2\theta (v_{\parallel}/v_{\perp})^2$. Since γ_L is significant only at large wave normal angles, we drop the J_1 term in (A.2). With the above approximations, (A.1) becomes

$$\frac{|\gamma_L|}{\omega} = \varepsilon \, \Phi(\theta, \omega/\Omega_+) \tag{A.10}$$

where the energy factor is

$$\varepsilon = -\pi v_{\parallel}^2 \int_0^{\infty} v_{\perp} \, dv_{\perp} \, \frac{\partial F}{\partial v_{\parallel}} \Big|_{v = \omega/k_{\parallel} = v_{ph}} \tag{A.11}$$

and the angular dependence is

$$\Phi(\theta, \omega/\Omega_+) = 4(\omega_{p_-}/\omega)^2 \, M^2/\rho \tag{A.12}$$

We now choose an isotropic Maxwellian distribution for the plasmaspheric electrons so that

$$F^-(v) = \left(\frac{1}{\sqrt{\pi} \, v_{th}} \right)^3 \exp\left[- \frac{(v_{\perp}^2 + v_{\parallel}^2)}{v_{th}^2} \right] \tag{A.13}$$

where $v_{th} = \sqrt{2T_E/M_-}$ is the electron thermal speed. (A.11) then reduces to

$$\varepsilon \left(\frac{v_{ph}}{v_{th}} \right) = \frac{1}{\sqrt{\pi}} \left(\frac{v_{ph}}{v_{th}} \right)^3 \exp\left[- \left(\frac{v_{ph}}{v_{th}} \right)^2 \right] \tag{A.14}$$

where the parallel phase velocity of ion cyclotron waves is

$$v_{ph} = v_A (1 - \omega/\Omega_+)^{1/2} \tag{A.15}$$

Near the magnetic equatorial plane we expect $v_{ph}/v_{th} \sim 1$ so that $\varepsilon(v_{ph}/v_{th}) \sim$ (1) . After some tedious algebraic manipulation, (A.12) can be written approximately as

$$\Phi(\delta) \simeq \frac{\delta^2}{(1 + \delta^2/2)(1 + \delta^2)^2} \qquad \text{(A.16)}$$

where

$$\delta = \tan\theta/\tan\theta_{res} \qquad \text{(A.17)}$$

Since the wave normal angle never actually approaches the resonance cone, $\delta << 1$, a reasonable approximation is to take $\Phi(\delta) \simeq \delta^2$. Substitution of (A.13) into (A.10) then yields

$$\frac{|\gamma_L|}{\omega} = \frac{1}{\sqrt{\pi}} \left[\frac{\tan\theta}{\tan\theta_{res}} \right]^2 \left(\frac{v_{ph}}{v_{th}} \right)^3 \exp\left[- \left(\frac{v_{ph}}{v_{th}} \right)^2 \right] \qquad \text{(A.18)}$$

ACKNOWLEDGMENTS

It is a pleasure to acknowledge many valuable discussions with Professor C. F. Kennel. We are grateful to Professor R. A. Helliwell for use of the Stanford ray tracing program.

This work was supported in part by the National Aeronautics and Space Administration, Grant NGR 05-007-190, Air Force contract F04701-68-C-0200, and UCLA Academic Senate grant 2525.

REFERENCES

Akasofu, S. I., Polar and Magnetospheric Substorms, Springer Verlag, New York, 1969.

Carpenter, D. L., "Whistler studies of the plasmapause in the magnetosphere. 1. Temporal variations in the position of the knee and some evidence on plasma motions near the knee," J. Geophys. Res., 71, 693, 1966.

Carpenter, D. L., "Whistler evidence of the dynamic behavior of the duskside bulge in the plasmasphere," J. Geophys. Res., 75, 3837, 1970.

Chandra, S., E. J. R. Maier, B. E. Troy, Jr., and B. C. Narasinga Rao "The mid-latitude red arc and the associated ionospheric phenomena," Trans. AGU, 57, 377, 1970.

Chappell, C. R., K. K. Harris, and G. W. Sharp, "The morphology of the bulge region of the plasmapause," J. Geophys. Res., 75, 3848, 1970.

Chappell, C. R., K. K. Harris, and G. W. Sharp, "OGO-V measurements of the plasmasphere during observations of stable auroral red arcs," J. Geophys. Res. 1970 (in press).

Clark, W. L., J. R. McAfee, R. B. Norton, and J. M. Warnoch, "Radio wave reflections from large horizontal gradients in the topside ionosphere," Proc. I.E.E.E., 57, 493, 1969.

Cocke, W. J., and J. M. Cornwall, "Theoretical simulation of micropulsation," J. Geophys. Res., 72, 2843, 1967.

Cole, K. D., "On the depletion of ionization in the outer magnetosphere during magnetic disturbances," J. Geophys. Res., 69, 3595, 1964.

Cole, K. D., "Stable auroral red arcs, sinks for energy of D_{st} main phase," J. Geophys. Res., 70, 1689, 1965.

Cole, K. D., "On the D_{st} main phase and certain associated phenomena," in Physics of Geomagnetic Phenomena, eds., S. Matsushita and W. H. Campbell, Academic Press, New York, 1967.

Cornwall, J. M., "Micropulsations and the outer radiation zone," J. Geophys. Res., 71, 2185, 1966.

Cornwall, J. M., F. V. Coroniti, and R. M. Thorne, "Turbulent loss of ring current protons," J. Geophys. Res., 75, 4699, 1970.

Coroniti, F. V., and C. F. Kennel, "Electron precipitation pulsations," J. Geophys. Res., 75, 1279, 1970.

Davis, L. R., and J. M. Williamson, "Outer zone protons," in Radiation Trapped in the Earth's Magnetic Field, ed. Billy M. McCormac, Reidel Publ. Co., Dordrecht, Holland, 1966.

Dobes, K., "The HM wave-particle cyclotron resonance for non-parallel propagation," Planet. Space Sci., 18, 395, 1970.

Eather, R. H., "Auroral proton precipitation and hydrogen emissions," Rev. Geophysics, 5, 207, 1967.

Eather, R. H., and R. L. Carovillano, "The ring current as the source for proton auroras," submitted to Cosmic Electrodynamics, 1970.

Elliott, D. D., and S. La Valle, unpublished, 1970.

Frank, L. A., "On the extraterrestrial ring current during geomagnetic storms," J. Geophys. Res., 72, 3753, 1967.

Frank, L. A., "Direct detection of asymmetric increases of extraterrestrial 'ring current' proton intensities in the outer radiation zone," J. Geophys. Res., 75, 1263, 1970.

Frank, L. A., and H. D. Owens, "Omnidirectional intensity contours of low-energy protons ($0.5 \leq E \leq 50$ keV) in the earth's outer radiation zone at the magnetic equator," J. Geophys. Res., 75, 1269, 1970.

Glass, N. W., J. H. Wolcott, L. W. Miller, and N. M. Robertson, "Local time behavior of the alignment and position of a SAR arc," J. Geophys. Res., (in press) 1970.

Gendrin, R., "Pitch angle diffusion of low energy protons due to gyroresonant interaction with hydromagnetic waves," J. Atmos. Terr. Phys., 30, 1313, 1968.

Haerendel, G., "On the balance between radial and pitch angle diffusion," in Particles and Fields in the Magnetosphere, ed. B. M. McCormac, Springer Verlag, New York, 1970.

Kennel, C. F., "Consequences of a magnetospheric plasma," Rev. Geophysics, 7, 379, 1969.

Kennel, C. F., and H. E. Petschek, "A limit on stably trapped particle fluxes," J. Geophys. Res., 71, 1, 1966.

Kennel, C. F., and H. V. Wong, "Resonantly unstable off-angle hydromagnetic waves," J. Plasma Phys., 1, 81, 1967.

Kitamura, T., and J. A. Jacobs, "Ray paths of Pc1 waves in the magnetosphere," Planet. Space Sci., 16, 863, 1968.

Nagy, A. F., R. G. Roble, and P. B. Hays, "Stable mid-latitude red arcs: observations and theory," Aeronomy report No. 3, University of Michigan College of Engineering, 1970.

Norton, R. B., and J. A. Findlay, "Electron temperature and density in the vicinity of the 29 September 1967 middle latitude red arc," Planet. Space Sci., 17, 1867, 1969.

Norton, R. B., and E. Marovich, "Alouette observations taken during a middle-latitude red arc," Proc. I.E.E.E., 57, 1158, 1969.

Prag, A. B., F. A. Morse, and R. J. McNeal, "Nightglow excitation and maintenance of the night-time ionosphere by low-energy protons," J. Geophys. Res., 71, 3141, 1967.

Rees, M. H., and S.-I. Akasofu, "On the association between subvisual red arcs and the D_{st} (H) decrease," Planet. Space Sci., 11, 105, 1963.

Roach, F. E., D. Barbier, and R. A. Duncan, "Observations of a 6300 Å arc in France, the United States, and Australia," Ann. Geophys., 18, 390, 1962.

Roach, F. E., and J. R. Roach, "Stable 6300 Å auroral arcs in mid-latitudes," Planet. Space Sci., 11, 523, 1963.

Roble, R. G., "A theoretical and experimental study of the stable mid-latitude red arc (SAR-arc)," Ph.D. thesis, University of Michigan, 1909.

Roble, R. G., P. B. Hays, and A. F. Nagy, "Photometric and interferometric observations of a mid-latitude stable auroral red arc," Planet. Space Sci., 18, 431, 1970.

Roble, R. G., P. B. Hays, and A. F. Nagy, "Comparison of calculated and observed features of a stable mid-latitude red arc," J. Geophys. Res. 75, 4261, 1970.

Russell, C. T., and R. M. Thorne, "On the structure of the inner magnetosphere," Cosmic Electrodynamics, 1, 67, 1970.

Rycroft, M. J., and S. J. Burnell, "Statistical analysis of movements of the ionospheric trough and the plasmapause," J. Geophys. Res., 75, 5600, 1970.

Sckopke, N., A general relation between the energy of trapped particles and the disturbance field near the earth," J. Geophys. Res., 71, 3125, 1966.

Spitzer, L., Jr., Physics of Fully Ionized Gases, Interscience Publishers, New York, 1962.

Thomas, J. O., and M. K. Andrews, "Transpolar exospheric plasma. 1. Plasmaspheric termination," J. Geophys. Res., 73, 7407, 1968.

Walker, J. C. G., and M. H. Rees, "Excitation of stable auroral red arcs at subauroral latitudes," Planet. Space Sci., 16, 915, 1968.

TABLE I

Data from Frank and Owens [1970], covering the storm of 9 July 1966. Energies are given in keV.

Energy Range	Flux (cm^{-2} sec^{-1})	Number Density (cm^{-3})	Energy Density (ergs cm^{-3})
$30 < E < 50$	4.0×10^{8}	1.5	9.6×10^{-8}
$16 < E < 25$	4.5×10^{8}	2.4	7.7×10^{-8}
$11 < E < 19$	4.0×10^{8}	2.5	6×10^{-8}
$7 < E < 12$	2.5×10^{8}	1.9	3×10^{-8}
$3 < E < 5$	1.0×10^{8}	1.2	6×10^{-9}
$1.1 < E < 1.8$	4.5×10^{7}	0.9	2×10^{-9}
$0.45 < E < 0.75$	6×10^{6}	0.2	2×10^{-10}
TOTAL	1.6×10^{9}	10.6	2.7×10^{-7}

FIGURE CAPTIONS

Figure 1. A review of the magnetic storm model presented by Cornwall, Coroniti, and Thorne [1970]. 5 to 50 keV protons injected from the magnetospheric tail during magnetic storm main phase become highly unstable and are precipitated just inside the plasmapause. During the storm recovery the slow outward expansion of the plasmasphere erodes the symmetric ring current along the inner edge.

Figure 2. The observed D_{st} vs. SAR-arc intensity points of Rees and Akasofu [1963] are compared to theoretical curves estimated from the total energy content of the ring current, assuming a 25% energy conversion efficiency over a time scale of one-half to one day.

Figure 3. The thermal electron Landau damping rate of ion cyclotron waves is plotted against latitude along a typical magnetospheric ray path for both diffusive equilibrum and gyrofrequency (N/B = const.) density models. The wave normal angle between the magnetic field and propagation vector is also shown.

Figure 4. Ray path integrated damping rates for both diffusive equilibrium (solid lines) and gyrofrequency (dotted lines) density models are used to plot the residual wave energy against electron temperature for various wave frequencies normalized to the equatorial proton gyrofrequency along the ray path.

Figure 5. The total electron heat flux to the ionosphere due to both proton Coulomb dissipation and Landau wave absorption is plotted against electron temperature. Intersection points with the collisionless "Strong diffusion" conduction curve specify the equilibrium equatorial electron temperature and SAR-arc intensity.

Figure 6. A synopsis of the energy transfer processes responsible for SAR-arc formation at the plasmapause.

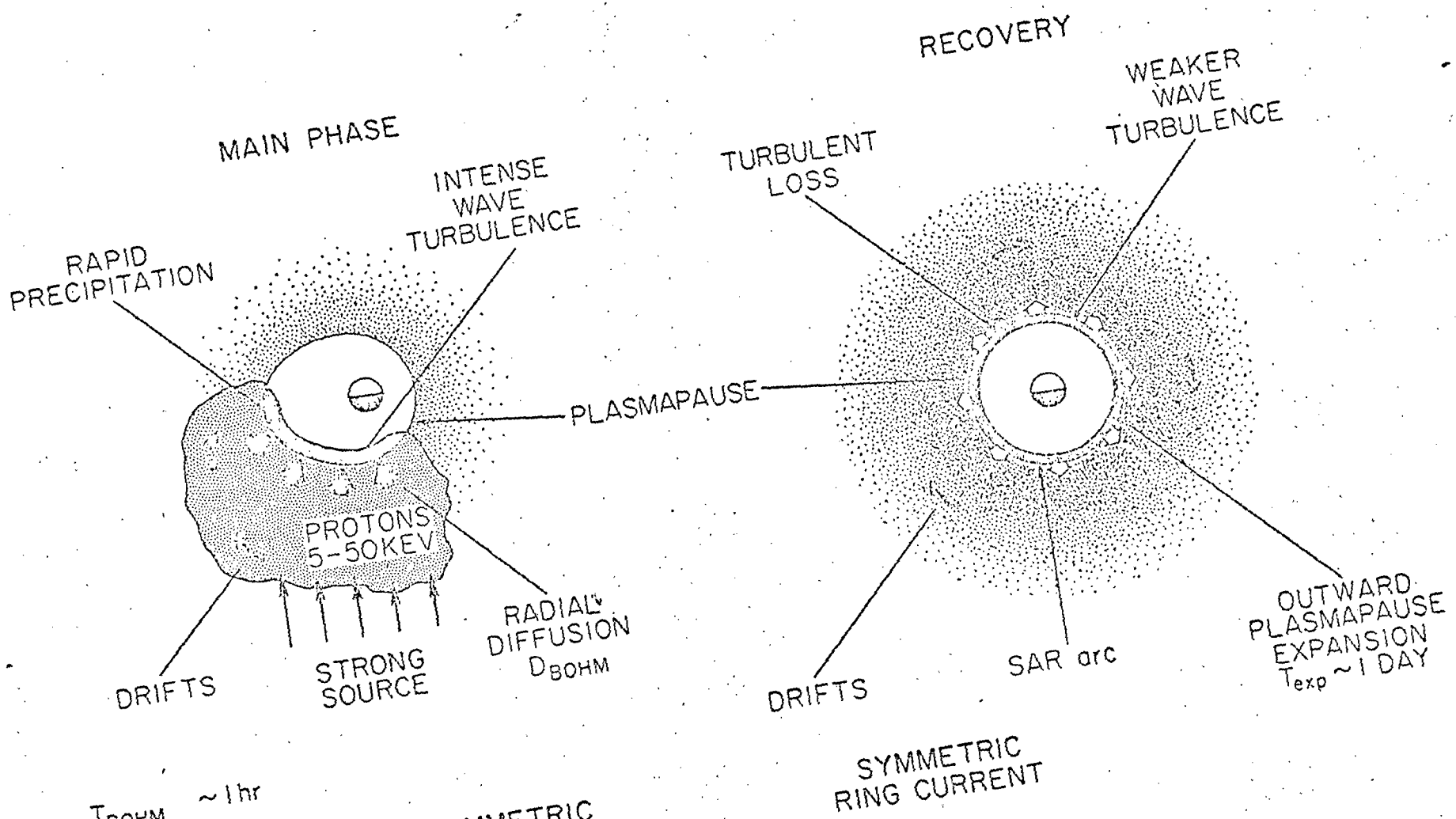

$T_{BOHM} \sim 1$ hr

$T_{MIN} \sim 1$ hr

$\frac{1}{4} T_{DRIFT} \sim 1$ hr

ASYMMETRIC RING CURRENT

SYMMETRIC RING CURRENT

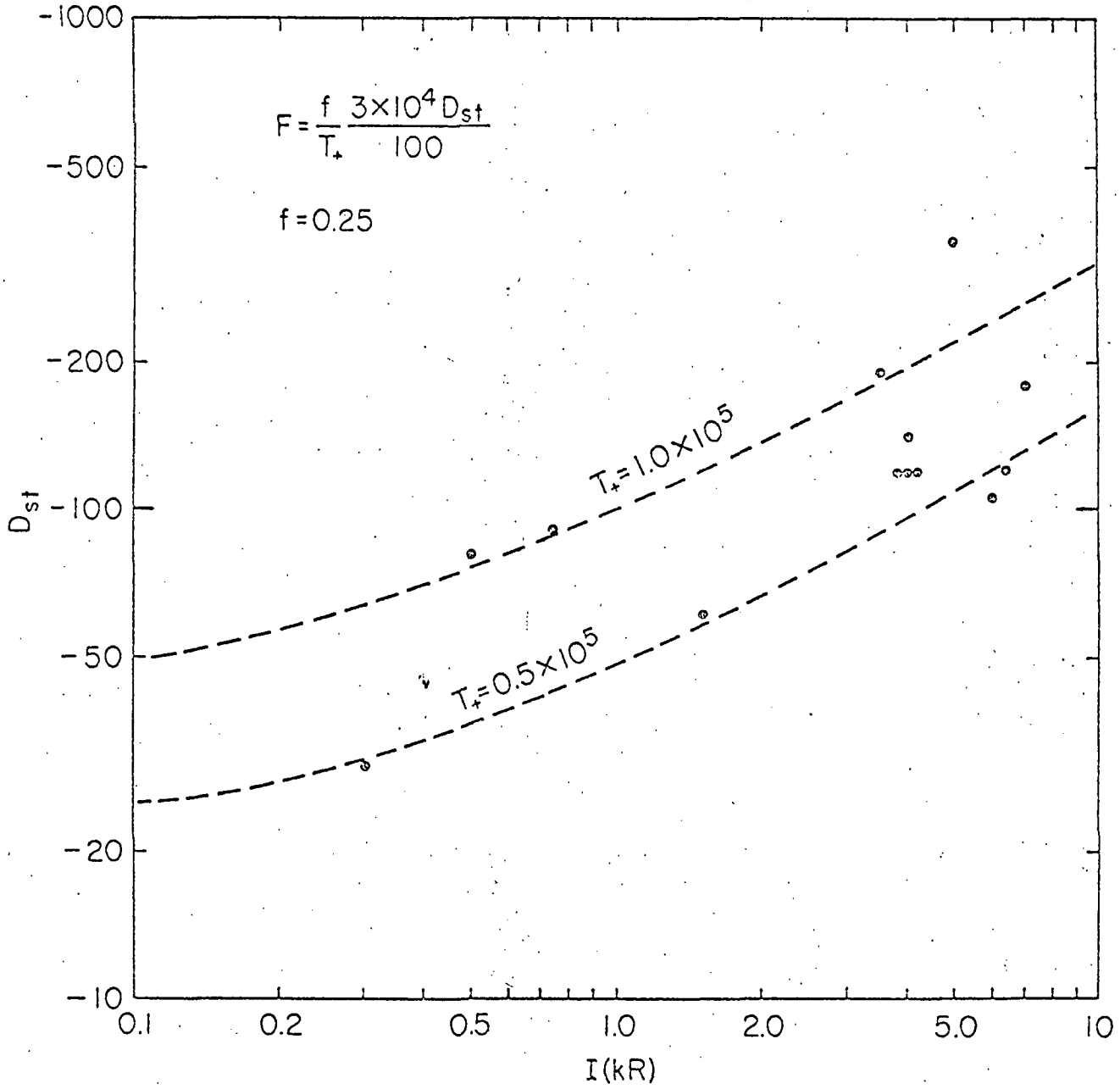
$F = \frac{f}{T_+} \frac{3\times10^4 D_{st}}{100}$
f = 0.25
$T_+ = 1.0\times10^5$
$T_+ = 0.5\times10^5$
D_{st}
-1000
-500
-200
-100
-50
-20
-10
0.1
0.2
0.5
1.0
2.0
5.0
10
I(kR)

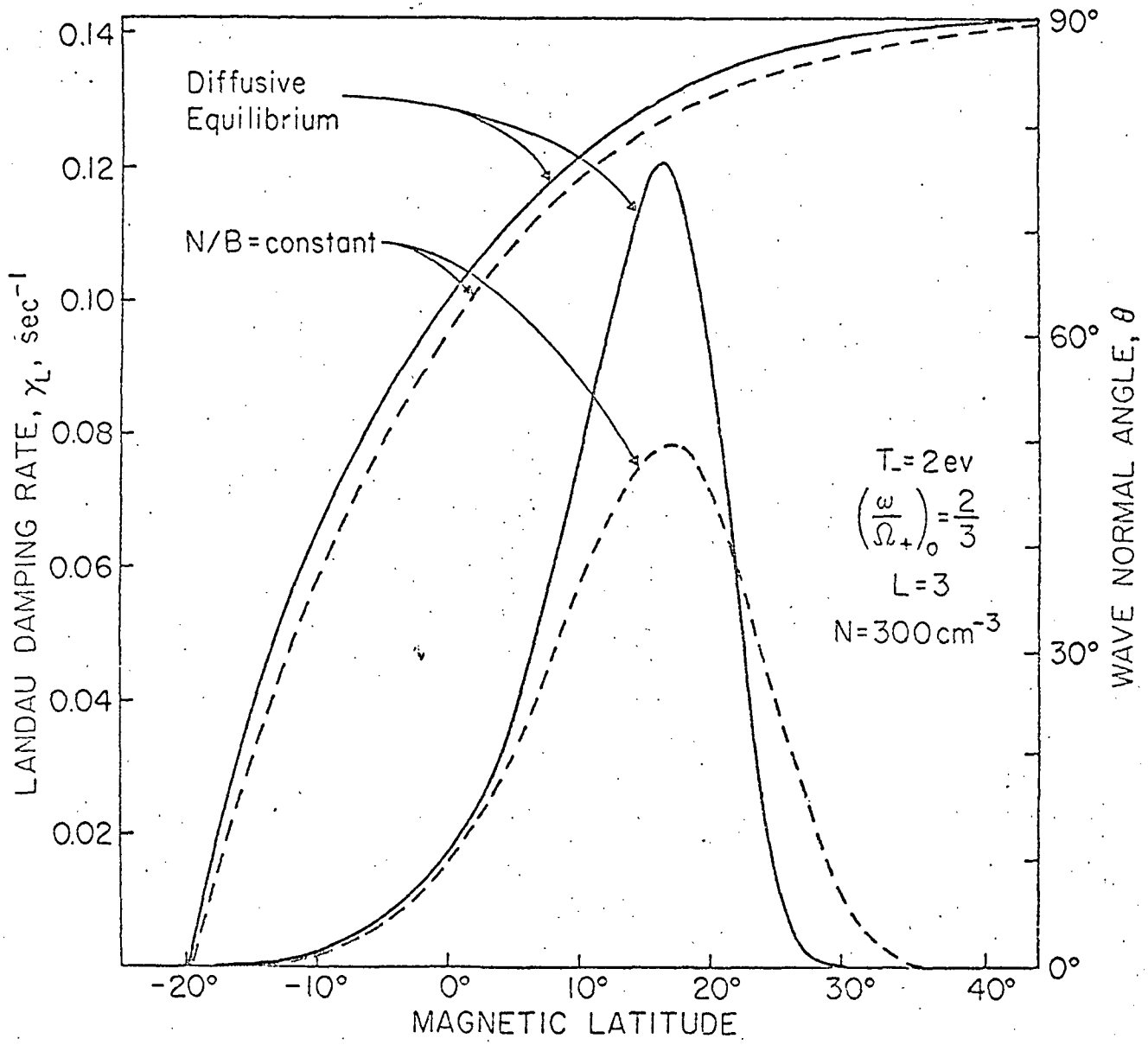
0.14
0.12
0.10
0.08
0.06
0.04
0.02
LANDAU DAMPING RATE, γ_L, sec^{-1}
Diffusive
Equilibrium
N/B = constant
$T_- = 2$ ev
$\left(\frac{\omega}{\Omega_+}\right)_0 = \frac{2}{3}$
L = 3
N = 300 cm^{-3}
90°
60°
30°
0°
WAVE NORMAL ANGLE, θ
-20°
-10°
0°
10°
20°
30°
40°
MAGNETIC LATITUDE

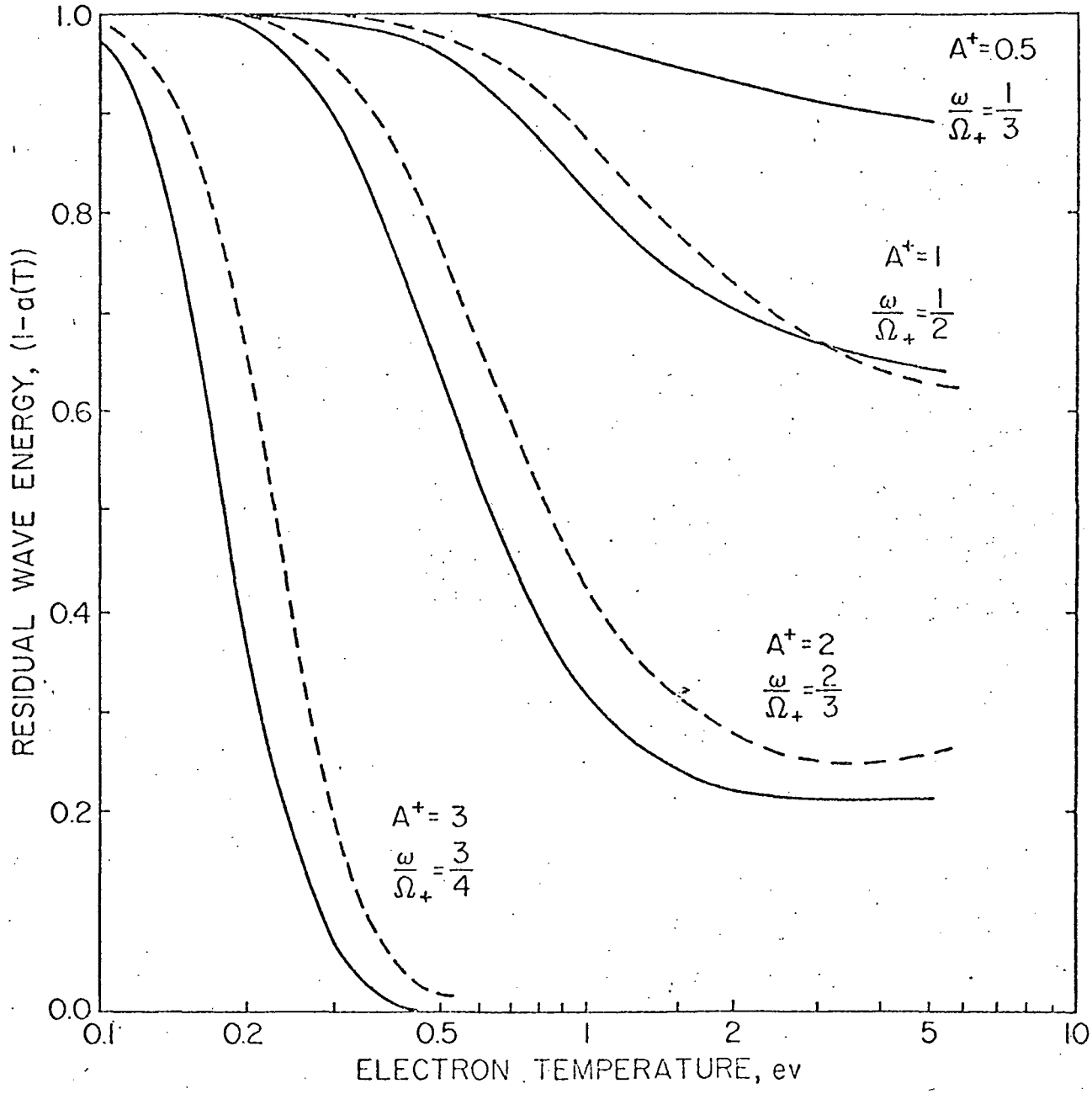
1.0
0.8
0.6
0.4
0.2
0.0
RESIDUAL WAVE ENERGY, (1-a(T))
0.1
0.2
0.5
1
2
5
10
ELECTRON TEMPERATURE, ev
A+=0.5
ω/Ω+ = 1/3
A+=1
ω/Ω+ = 1/2
A+=2
ω/Ω+ = 2/3
A+=3
ω/Ω+ = 3/4

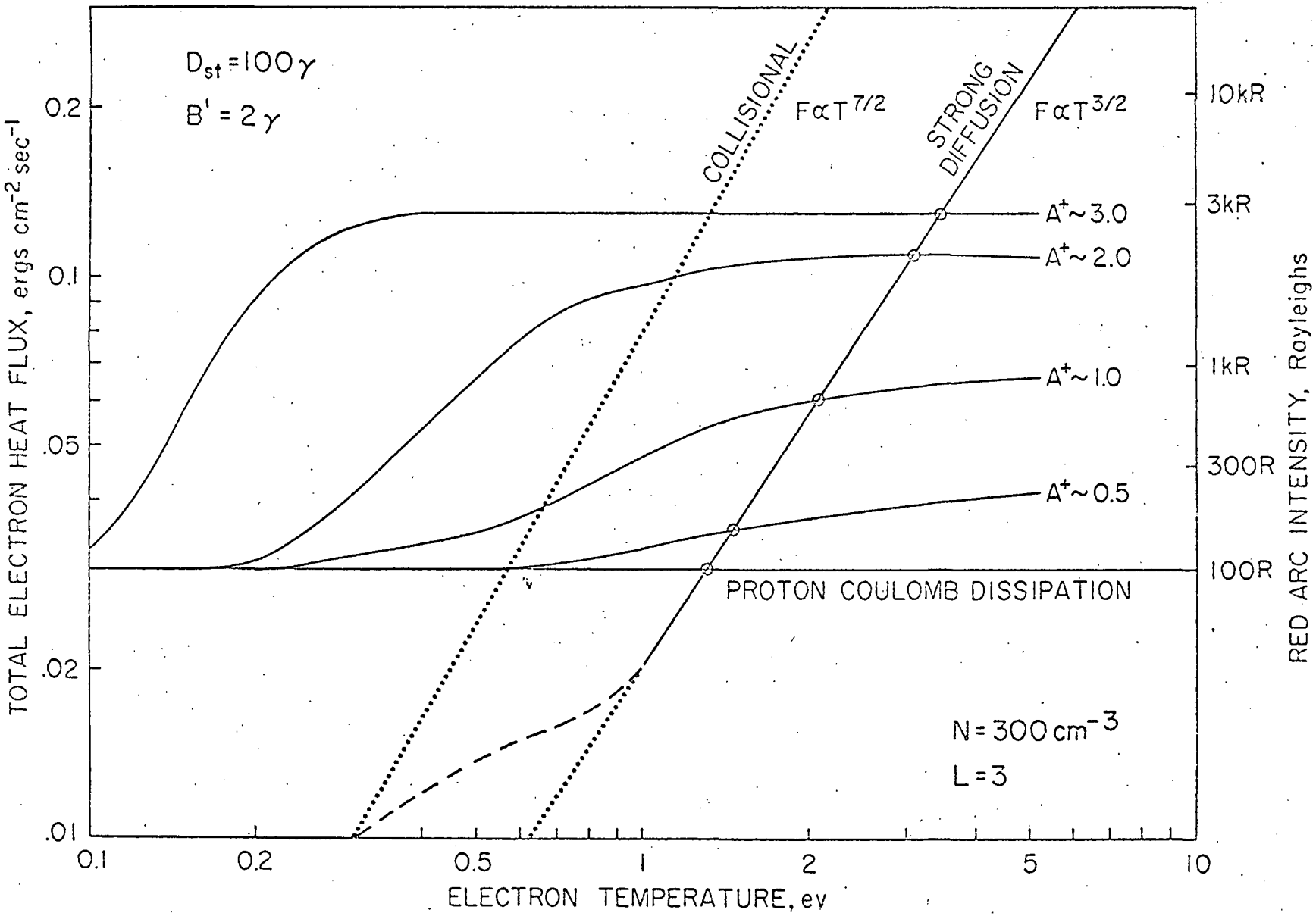
D_{st} = 100 γ
B' = 2 γ
COLLISIONAL
F∝T 7/2
STRONG DIFFUSION
F∝T 3/2
A+~3.0
A+~2.0
A+~1.0
A+~0.5
PROTON COULOMB DISSIPATION
N = 300 cm-3
L = 3
TOTAL ELECTRON HEAT FLUX, ergs cm-2 sec-1
ELECTRON TEMPERATURE, ev
RED ARC INTENSITY, Rayleighs
0.2
0.1
.05
.02
.01
0.1
0.2
0.5
1
2
5
10
10kR
3kR
1kR
300R
100R

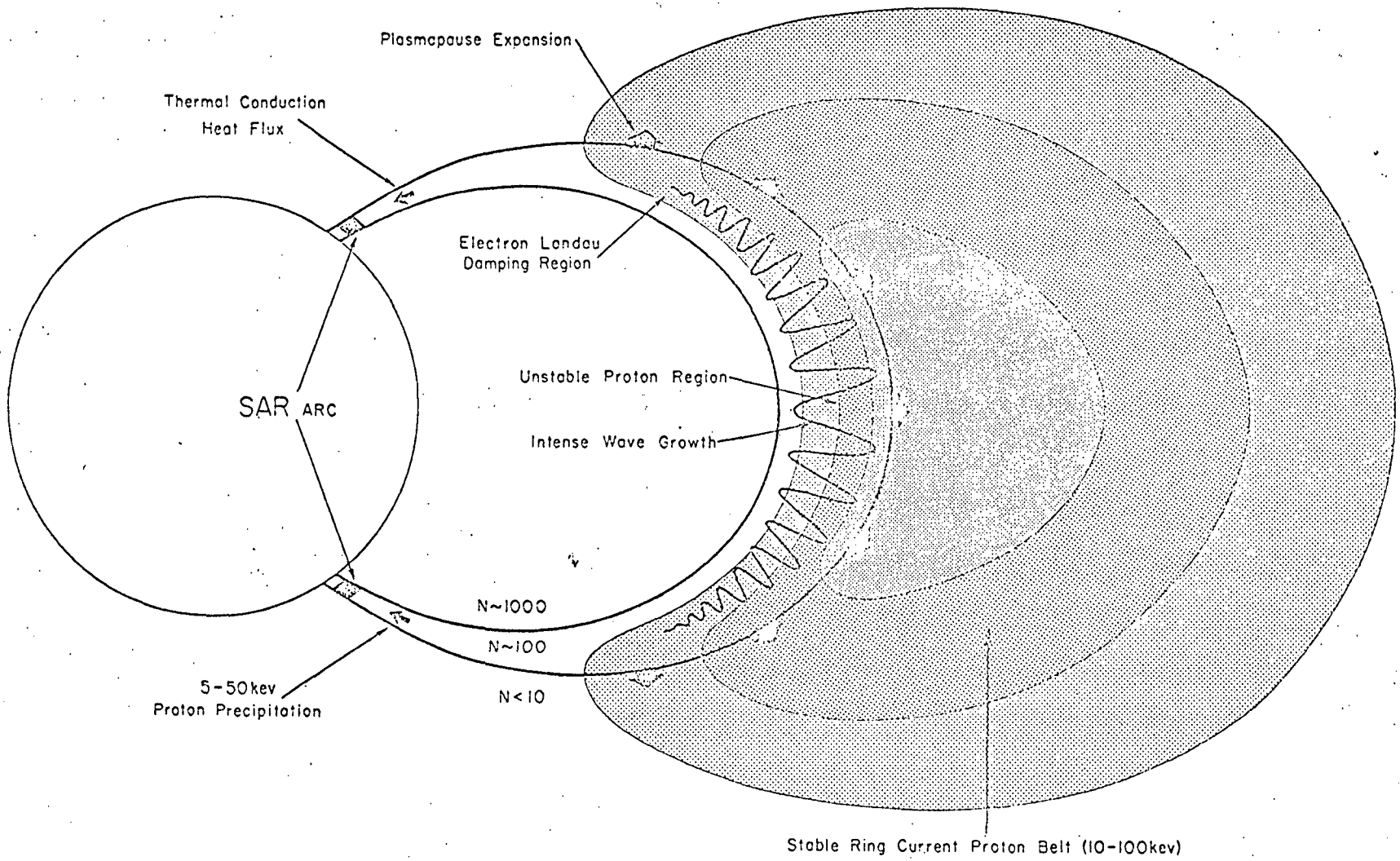
Plasmapause Expansion
Thermal Conduction
Heat Flux
Electron Landau
Damping Region
Unstable Proton Region
Intense Wave Growth
SAR ARC
N~1000
N~100
N<10
5-50kev
Proton Precipitation
Stable Ring Current Proton Belt (10-100kev)